# Solvent Effects on Nuclear Shieldings: Continuum or Discrete Solvation Models To Treat Hydrogen Bond and Polarity Effects?

**Benedetta Mennucci, José M. Martínez,† and Jacopo Tomasi***

*Dipartimento di Chimica e Chimica Industriale, Università di Pisa, via Risorgimento 35, 56126 Pisa, Italy*

*Received: March 5, 2001; In Final Form: May 11, 2001*

This paper presents a study on the effects of solvents on nuclear magnetic shielding parameters derived from NMR spectroscopy. In particular, the study focuses on a specific nucleus, nitrogen, in two molecular solutes, acetonitrile and pyridine, immersed in different solvents. Among the solvents, particular attention is devoted to chloroform; its specific characteristics (low polarity and proticity), in fact, make it a very challenging application for theoretical solvation models. Here, we exploit a coupling scheme of solute−solvent cluster structures generated through MD simulations and high-level quantum chemical calculations in which a continuum solvation model is also introduced. This scheme permits the study of the competitive effects due to short-range and highly directional H-bonds and to long-range electrostatic forces and of the way these two effects are taken into account through a discrete, a continuum, or a coupled description of the solvent. Natural bond analysis of computed results has been used to provide insight into the role of solvent-induced modifications of electronic distribution charge in the observed gas-to-solvent shift.

## 1. Introduction

The effects of solvent on nuclear magnetic shielding parameters derived from NMR spectroscopy have been of great interest for a long time. In 1960, Buckingham et al.[1] suggested a possible classification in terms of various additive corrections to the shielding arising from (i) the bulk magnetic susceptibility of the solvent, (ii) the magnetic anisotropy of the solvent molecules, (iii) van der Waals interactions, and (iv) long-range electrostatic interactions. In the original scheme, strong specific interactions, such as those acting in intermolecular hydrogen bonds, were not dealt with but just mentioned as a possible extreme form of the electrostatic or, more generally, "polar" effect; in the numerous applications which followed Buckingham's classification, however, this further effect has always been included as a separate contribution.

In general, it is possible to correct experimental data for the bulk susceptibility (i.e., to eliminate effects due to item i according to Buckingham's analysis), but there is no way to extract the remaining four effects which, in principle, are included in any measurement. For this reason, they have been the subject of several investigations even if not completely satisfactory rationalizations have been obtained so far. The widely believed idea is that short-range interactions can be effectively handled by supermolecule (or discrete) calculations involving a solute surrounded by a number of explicitly treated solvent molecules,[2] while reaction field (or continuum) methods generally provide an effective alternative to describe long-range electrostatic interactions.[3−5] As a result, the combination of the two approaches when coupled to accurate quantum mechanical methods should give an effective computational tool to include solvent effects into nuclear shielding calculations.

In this paper, we give a contribution to this topic by computing an articulate study on solvent effects on a specific nucleus, the nitrogen, using a nonstandard combination of schemes of different solvation models but always involving accurate ab initio calculations. The choice of nitrogen as the NMR active nucleus has been induced by the well-known sensitivity of its shielding to changes in the environment;[6] in particular, such sensitivity has been used as a probe of intermolecular forces and intramolecular force fields to provide information on the intramolecular potential of a given molecule as well as the intermolecular potential between two molecules and on the structure of fluids and solutions.

As a test application, we have selected a particular solute−solvent couple: a solute in which the nitrogen atom is involved in triple or aromatic double bonds (here, in particular, we have selected acetonitrile, $CH_3CN$, and pyridine, $C_5NH_5$) and a low−medium polar and protic solvent, namely chloroform, $CHCl_3$ (dielectric constant $\epsilon = 4.90$). The choice of these two solutes has been dictated by the fact that for both molecules, solvent-induced deformation of the electronic charge distribution should be significant and thus accurate ab initio methods become compulsory in order to obtain a proper description of solvent effects on the shielding. Regarding the solvent, $CHCl_3$ is a good choice for testing solvation models as, if we apply Buckingham's scheme, both "polar" contributions, i.e., electrostatic forces and H-bonding, should be equally active and dominant on the others; this selected multi-interaction behavior represents a challenging test for combined discrete−continuum solvation models. On the contrary, the same solvation schemes can be hardly applied to very apolar and nonprotic solvents for which weak van der Waals interactions, not sufficiently well reproduced by either supermolecule or continuum approaches, are likely to dominate. For completely opposite reasons, highly polar protic solvents (as water) are also of less interest, as in this case, the combination of small H-bonded clusters immersed in a continuum solvent should well represent the real solvent effects.

The study will be organized as follows: In the first part, we shall describe the theoretical methods used (continuum model + molecular dynamics) and the criteria applied to choose the

* To whom correspondence should be addressed. Electronic mail: tomasi@dcci.unipi.it.

† On leave from Departamento de Química Física, Universidad de Sevilla, Facultad de Química, Sevilla 41012, Spain.

10.1021/jp010837w CCC: $20.00 
Published on Web 07/07/2001

configurations to be used later on in the supermolecule ab initio computations. The rest of the paper will be devoted to present and discuss the results obtained for the property of interest (nitrogen nuclear shielding). Initially, we shall consider acetonitrile as solute and compute its gas-phase and solvated shielding (in three different solvents: cyclohexane, $CHCl_3$, and water) using an electrostatic-only solvation continuum model (the new version of the polarizable continuum model, PCM,[7] known by the acronym IEF−PCM[9]). Successively, we shall focus on a single specific solvent, $CHCl_3$, and shift to a supermolecule model (with or without the continuum) in which the solute−solvent clusters are obtained from molecular dynamics simulations: both flexible and rigid approaches will be tested. Next, a similar study will be repeated on pyridine as solute. For both solutes, an orbital-based study exploiting a NBO analysis will be used to rationalize the computed results.

## 2. Computational Methods

**2.1. IEF−PCM Solvation Continuum Model.** In the IEF−PCM model, the solvent is represented by a homogeneous continuum medium which is polarized by the solute placed in a cavity built in the bulk of the dielectric. The solute−solvent interactions are described in terms of a solvent reaction potential. The basic hypothesis is that one can always define a new energetic functional, the free energy $G$, depending on the solute electronic wave function

$$G(\Psi) = \langle \Psi | \hat{H}^0 | \Psi \rangle + \left\langle \Psi \left| \frac{1}{2} \hat{V}^R \right| \Psi \right\rangle \tag{1}$$

where $\hat{H}^0$ is the Hamiltonian describing the isolated molecule and $\hat{V}^R$ represents the solvent reaction operator. By applying the variational principle to this functional, we can derive the nonlinear Schrödinger equation specific for the solvated system.

In general, the computational strategy formulated to define the reaction potential is based on a modelization of the solvent interactions according to the theory of intermolecular forces. Within this framework, the energetic quantity $G$ and the corresponding reaction operator $\hat{V}^R$ are written as a sum of contributions of different physical origin related to dispersion, repulsion, and electrostatic forces between solute and solvent molecules. In the present paper, however, we shall consider the electrostatic part of the interactions only.

The electrostatic problem of a charge distribution, $\rho_M$, embedded in a cavity, C, (within which the permittivity is assumed to be equal to 1) surrounded by an isotropic continuum dielectric with a given permittivity, $\epsilon$, can be expressed as follows:

$$\begin{cases} -\Delta V = 4\pi\rho_M & \text{in C} \\ -\epsilon\Delta V = 0 & \text{outside C} \\ [V] = 0 & \text{on } \Sigma \\ [\partial_x V] = 0 & \text{on } \Sigma \end{cases} \tag{2}$$

where $V$ indicates the electrostatic potential and $\Sigma$ is the cavity surface. The jump condition, $[V] = 0$, means that the potential $V$ is continuous across the interface $\Sigma$, i.e., $V_e - V_i = 0$ on $\Sigma$ where the subscripts e and i indicate the exterior and the interior of the molecular cavity, respectively. The equality $[\partial_x V] = 0$ is a formal expression of the jump condition of the gradient of the potential; for a homogeneous isotropic dielectric, it takes the well-known form

$$\left(\frac{\partial V}{\partial n}\right)_i - \epsilon\left(\frac{\partial V}{\partial n}\right)_e = 0 \tag{3}$$

where $n$ is the outward pointing unit vector perpendicular to the cavity.

Within the integral equation formalism (IEF),[9] one can transform the first two equations in system 2 into integral equations on the surface $\Sigma$ that can be solved with standard numerical methods. The solution of system 2 is thus reduced to a sum of two electrostatic potentials, one produced by $\rho_M$ in vacuo and the other due to a surface charge distribution $\sigma$ placed on the interface which arises from the polarization of the dielectric medium:

$$V(x) = V_M(x) + V_\sigma(x) = \int_{R^3} \frac{\rho_M(y)}{|x-y|}\,dy + \int_\Sigma \frac{\sigma(s)}{|x-s|}\,ds \tag{4}$$

where the integral in the first term is taken over the entire three-dimensional space. The problem is then shifted to the definition of the proper apparent surface charge (ASC), $\sigma$. In computational practice, use is made of a partition of the cavity surface into small regions, called tesserae, with known area, $a_k$. In the limit of a sufficiently accurate mapping, one can always approximate the continuum distribution $\sigma$ on each tessera with a single-value quantity to define the equivalent sets of pointlike charges as $q(s_k) = \sigma(s_k)a_k$ where $s_k$ indicates the representative point of tessera $k$ (i.e., the point at which we compute $\sigma$).

In this scheme, the reaction potential, $\hat{V}^R$, to be introduced in the effective Hamiltonian is reduced to one-electron operators depending on $q(s_k)$, and thus, the IEF−PCM method can be straightforwardly applied to different levels of the quantum mechanical description and modeled to include various concepts and approaches provided by the general quantum mechanical theory. The important new aspect to be taken into account is the introduction of an additional nonlinear character not present in isolated systems; the apparent charges, $q(s_k)$, depend on the solute charge distribution they contribute to modify.

*2.1.1. Nuclear Shielding for an IEF Solute.* For a molecular solute, the nuclear magnetic shielding tensor $\boldsymbol{\sigma}^X$ of a nucleus, X, is expressed as mixed second derivatives of the free energy functional, $G$, with respect to the external magnetic field, $B$, and the nuclear magnetic moment, $\mu^X$,

$$\sigma_{ij}^X = \frac{\partial^2 G}{\partial B_i\, \partial \mu_j^X} \tag{5}$$

where $B_i$ and $\mu_j^X$ ($i, j = x, y, z$) are the Cartesian components of the external magnetic field, $B$, and of the nuclear magnetic moment, $\mu^X$, respectively.

The presence of the magnetic field introduces the problem of the definition of the origin of the corresponding vector potential. However, because $\sigma$ is a molecular property, it must be invariant with respect to changes of the gauge origin. To obtain this gauge invariance in the ab initio calculations, one can introduce gauge factors into the atomic orbitals of the basis set in such a manner that the results are independent of the gauge origin even though the calculation is approximate. Inclusion of gauge factors in the atomic orbitals may be accomplished by using gauge invariant atomic orbitals (GIAO)[8]

$$\chi_\nu(B) = \chi_\nu(0)\exp\left[-\frac{i}{2c}(B \times R_\nu)\cdot r\right] \tag{6}$$

where $R_\nu$ is the position vector of the basis function, and $\chi_\nu(0)$ denotes the usual field-independent basis function.

The GIAO method is used in conjunction with analytical derivative theory; in this approach, the magnetic field perturbation is treated in an analogous way to the perturbation produced

by changes in the nuclear coordinates. For a solute described at Hartree−Fock or DFT level with expansion of the molecular orbitals over the previously defined field-dependent basis set, the components of the nuclear magnetic shielding tensor are obtained as

$$\sigma_{ij}^{X} = \mathrm{tr}[\mathbf{P}\mathbf{h}^{B_i\mu_j^X} + \mathbf{P}^{B_i}\mathbf{h}^{\mu_j^X}] \quad (7)$$

where $\mathbf{P}^{B_i}$ is the derivative of the density matrix with respect to the magnetic field. Matrices $\mathbf{h}^{\mu_j^X}$ and $\mathbf{h}^{B_i\mu_j^X}$ contain the first derivative of the standard one-electron Hamiltonian with respect to the nuclear magnetic moment and the second derivative with respect the magnetic field and the nuclear magnetic moment, respectively. Both terms do not contain explicit solvent-induced contributions as these contributions do not depend on the nuclear magnetic moment of the solute and thus the corresponding derivatives are zero. On the contrary, explicit solvent effects act on the first derivative of the density matrix $\mathbf{P}^B$ which can be obtained as solution of the corresponding first-order coupled−perturbed HF (or Kohn−Sham, KS) equation.[5]

**2.2. Molecular Dynamics Calculations.** Molecular dynamics simulations were performed with the DL_POLY 2.12 package[10] in the microcanonical ensemble and using periodic boundary conditions. For the simulations containing acetonitrile as solute, the recent model of Grabuleda et al.[12] was employed, while solvent chloroform molecules were described by the parametrization performed by Fox and Kollman.[11] In both cases, potential parameters were developed in the framework of the Cornell et al.[13] force field providing flexible all-atom models for both type of molecules. Internal deformations were allowed by means of the usual bond, angle, and torsion terms, while the nonbonded van der Waals and electrostatic ones were used to describe the intermolecular interactions. Two types of simulations, as indicated below, were performed for the chloroform solution of acetonitrile. In one case, flexibility was allowed in both solute and solvent molecules and only bonds involving hydrogen atoms were constrained to their equilibrium values by means of the SHAKE[14] algorithm. A second simulation was performed in which all molecules were treated as rigid bodies at their equilibrium geometries and only intermolecular interactions were considered. For the pyridine study, the Jorgensen and McDonald[15] all-atom force field was employed. This force field allows internal deformations as well for the heterocycle, but in this case, only rigid solute and $CHCl_3$ solvent molecules were considered in the corresponding MD simulation.

All simulations contained one solute (acetonitrile or pyridine) molecule and 256 solvent, chloroform, molecules. To set up the systems, a cubic box containing 258 solvent molecules was equilibrated at 298 K. The experimental density,[19] 1.473 g/cm$^3$, was used to establish box sides ($L$). Solutes were introduced by replacing two adjacent solvent molecules in the equilibrated box with the solute molecule. After initial minimization to remove bad contacts when necessary, systems were thermalized at 298 K. Production periods of 300 and 150 ps for the simulations containing rigid and flexible models, respectively, were obtained. Equations of motions were integrated with time steps of 2 and 0.25 fs for the rigid and flexible cases, respectively. In the first case, rigid bodies were treated by the quaternion formalism[16] and an implicit leapfrog quaternion algorithm[17] was applied. When dealing with flexible molecules, Verlet leapfrog scheme[18] was employed. Coulombic interactions were computed using the Ewald sum technique,[18] and a spherical molecular cutoff of $L/2$ was applied for the short-range interactions.

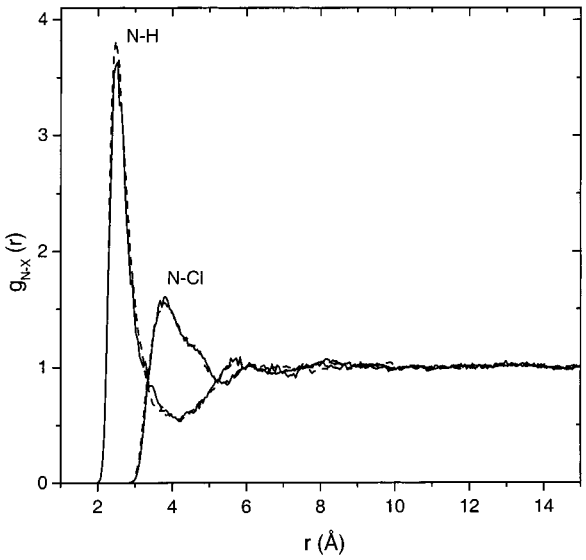


**Figure 1.** Radial distribution functions for the N−H and N−Cl pairs in the chloroform solutions of acetonitrile. Solid and dashed lines correspond to simulations using the rigid and flexible models, respectively.

*2.2.1. Radial Distribution Functions and Selection of Structures.* In the context of statistical simulations, primary information regarding the structure of the solvent in the nearest neighborhood of the solute may be obtained by means of the radial distribution functions (RDFs). This information will be used in this work to define in a consistent way the size of the clusters used in the ab initio calculations. As nuclear shieldings will be computed on the nitrogen atom of acetonitrile and pyridine, initially, the RDFs of interest will be those centered on this solute atom. Figure 1 shows the N−Cl and N−H RDFs obtained for the two simulations performed of acetonitrile in chloroform.

The first fact to notice is the marginal effect of freezing the molecules when passing from the flexible to the rigid models on the distributions obtained. In fact, with the present statistical noise, longer simulation times are needed to establish the origin of the observed differences. It can be inferred from $g_{N-Cl}$ and $g_{N-H}$ distributions that chloroform molecules around the nitrogen atom of the acetonitrile have a preferential orientation with the hydrogen atom oriented toward the N center.

A well-defined first peak centered at ca. 2.50 Å is observed (see Figure 1) for the N−H pair distribution, locating the first minimum at 4.2 Å. The corresponding running integration number up to this value is 4.2.

In the case of the pyridine solution, Figure 2, the situation is similar although first peaks are no so well defined, showing a more diffuse distribution of chloroform molecules in the neighborhood of the N atom.

In this case, the minimum in the $g_{N-H}$ is not as well defined as in the acetonitrile case, but a reasonable value to define the closest shell of hydrogen atoms can be located in the range of 3.7−4.0 Å, yielding integration numbers between 1.5 and 1.8.

With the information supplied from the computed RDFs, the selection of the solvent molecules included in a given cluster is done on the basis of a cutoff distance ($r_{cut}$) for the N−H pair: all solvent molecules having the hydrogen atom closer than $r_{cut}$ to the solute nitrogen will be included in the NMR ab initio calculation of the corresponding structure. Values used for $r_{cut}$ are 4.2 and 3.8 Å for the acetonitrile and pyridine simulations, respectively. With this criterion, sets of structures were generated for the different simulations, the separation

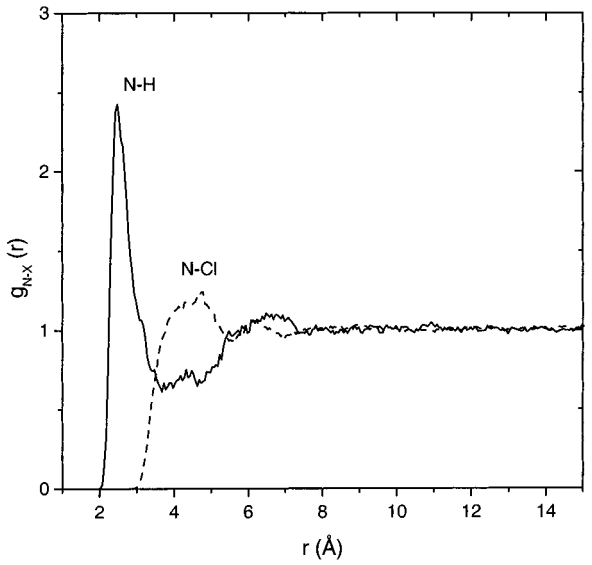


**Figure 2.** Radial distribution functions for the N−H and N−Cl pairs in the chloroform solution of pyridine.

between two consecutive structures in a given set being 10 ps. This large time separation avoids any kind of correlation in the structures selected, so a proper sampling can be performed on the basis of the configurations used. Two examples of the type of clusters generated are shown in Figure 3 for the simulations with rigid molecules of acetonitrile and pyridine.

### 3. Results and Discussions

The present section will be mainly focused on the analysis of N nuclear shielding of acetonitrile in $CHCl_3$ (some results are also reported for cyclohexane and water as solvents); the parallel analysis on pyridine will be less detailed and used more as a counterexample with respect to acetonitrile than as an independent study.

Solvated systems will be represented both in the framework of the IEF−PCM electrostatic continuum model and in that of a supermolecule approach (eventually including the continuum). For the supermolecule calculations, the solute−solvent cluster structures have been obtained through MD simulations (see previous section for details).

In the calculation of nuclear shieldings, fixed experimental geometries have been used both in the gas phase and in the presence of the solvent. To take into account the gauge-origin problem, we have used the gauge-including atomic orbital (GIAO) method[8] at density functional level of theory.[20] All ab initio calculations both in vacuo and in solution have been performed using a development version of the Gaussian code.[21]

Before starting the study of solvated systems, let us check the quantum mechanical level of calculation we shall exploit in the following analysis; for this preliminary step, we limit the calculations to the isolated systems only.

**3.1. Basis Set Dependence of Nuclear Shielding.** Some exploration on the effect of basis sets and of the density functional on the calculated gas-phase nitrogen absolute shielding in $CH_3CN$ and pyridine is reported in Table 1.

There are large changes of about 30−40 ppm upon expanding the valence representation from double-ζ 6-31+G(d,p) to triple-ζ 6-311+G(d,p), while upon adding more polarization functions and/or diffuse functions no significant changes are found.

Passing to the effect of changing the functional, two alternatives have been considered, namely, the B3LYP and the MPW1PW91:[22] the former has been considered because it is one of the most used functionals and also because it has shown good behaviors in many different applications (including nuclear shielding calculations); the second one has been tested, even if much less used than B3LYP, because of its successful application in shielding calculations on C.[23] From what is reported in Table 1, it is clear that no significant differences can be obtained from these functionals.

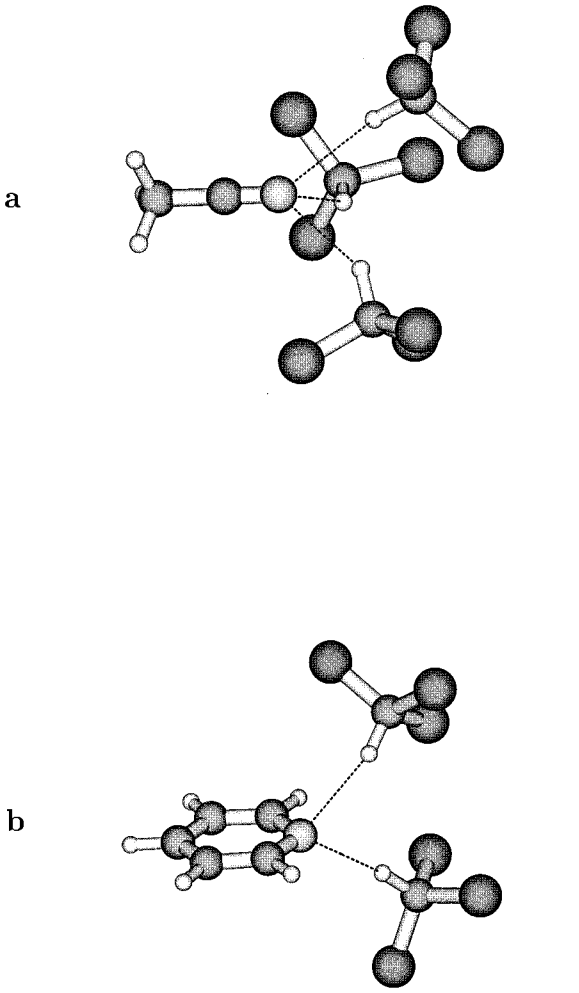


**Figure 3.** Two examples of the acetonitrile−chloroform (a) and pyridine−chloroform (b) clusters used in the ONIOM computations of Table 3.

**TABLE 1: Effect of Basis Set and Functional on Gas-Phase N Nuclear Shielding (in ppm) of Acetonitrile and Pyridine**

| | $CH_3CN$ | | PYRIDINE | |
|---|---|---|---|---|
| | B3LYP | MPW1PW91 | B3LYP | MPW1PW91 |
| 6-31+G(d,p) | 10.47 | 8.67 | −63.14 | −60.91 |
| 6-311+G(d,p) | −25.51 | −24.06 | −102.78 | −96.95 |
| 6-311+G(2d,2p) | −25.82 | −24.29 | −101.36 | −95.66 |
| 6-311++G(2d,2p) | −25.83 | −24.27 | −101.38 | −95.68 |

In any case, i.e., with any basis set/functional combination, significant differences are found with respect to the experimental data: −8.7 ppm for $CH_3CN$ and −81.8 for pyridine.[6] This fact, however, is not crucial in this study as solvent-induced shifts are to be computed, and thus, eventual inadequacies of the quantum mechanical level of calculations will be, to a large extent, canceled in the difference between the gas-phase reference and solvent-including calculations. On the basis of these considerations, it has been decided to use B3LYP as functional and 6-311+G(d,p) as basis for following calculations on all the systems in this study.

**TABLE 2: IEF−PCM Computed N Nuclear Shielding ($\sigma$(N) in ppm) and Gas-to-Solution Shift ($\Delta\sigma$(N)) for Acetonitrile in Various Solvents with Respect to the Cavity Size Here Represented by the Scaling Factor *f***

| | $\sigma$(N) | | | $\Delta\sigma$(N) | | |
|---|---|---|---|---|---|---|
| *f* | cyclohexane | $CHCl_3$ | WATER | cyclohexane | $CHCl_3$ | WATER |
| 1.2 | −15.64 | −7.79 | −1.25 | −9.86 | −17.72 | −24.26 |
| 1.4 | −18.53 | −13.12 | −8.72 | −6.98 | −12.39 | −16.79 |
| 1.6 | −20.47 | −16.62 | −13.54 | −5.04 | −8.89 | −11.97 |
| 1.2/1.2/1.6 | −17.97 | −11.96 | −6.97 | −7.54 | −13.55 | −18.85 |
| 1.2/1.6/1.6 | −18.55 | −12.80 | −7.86 | −6.96 | −12.71 | −17.94 |
| 1.6/1.2/1.2 | −18.60 | −13.30 | −8.99 | −6.91 | −12.21 | −16.52 |
| exptl[a] | | | | +2.5 | −6.2 | −17.2 |

[a] Reference 6.

**3.2. Acetonitrile.** *3.2.1. Cavity Size Effect.* The importance of the cavity definition in continuum solvation methods is a well-known aspect which has led to many different studies of systematic nature.[24] Since its original version, PCM defines the cavity as an envelope of spheres centered on atoms (or at most atomic groups); here, we maintain the same feature for all the numerical calculations. By the adoption of this definition, the problem is shifted to the size of the spheres; although several computations have shown that standard van der Waals radii provide reasonable cavity sizes, a number of improvements have been suggested.[25] In the present application, we define the cavity in terms of spheres centered on some selected atoms and with radii, $R_A$, proportional to van der Waals radii:

$$R_A = fR_A^{vdW}$$

The initially proposed factor for the evaluation of the electrostatic contribution to the solvation free energy of neutral solutes was $f = 1.2$. The occurrence of a scaling factor larger than 1 is justified by considering that atomic bond or lone pair charge centers of the solvent molecules are normally located a bit further from the solute atoms than a van der Waals radius. The value $f = 1.2$ was chosen on the basis of the energy decomposition analysis over a few sets of cluster systems.[24] From this first proposal, many studies have been done on the choice of the best scaling factor; however, the value 1.2, at least for neutral molecules in aqueous solution, has always been confirmed as a valid one.

Until now, however, all the main tests have been focused on energy considerations; in other words, the leading aspect commonly adopted is the search of the best agreement between computed and experimental solvation free energy values. This is clearly a very important feature to be fulfilled for any accurate and reliable solvation method, but other aspects should also be considered. In particular, it may happen that a cavity which gives the best values of solvation free energies is not good enough when we pass to consider other molecular properties. In this paper, we give an alternative analysis choosing, as a test quantity, the isotropic nuclear magnetic shielding, $\sigma$.

In Table 2 we report the absolute N nuclear shielding, $\sigma$, and the gas-to-solution shift, $\Delta\sigma = \sigma_{vac} - \sigma_{sol}$, computed at B3LYP/6-311+G(d,p) level with respect to the cavity size, here represented by the value of the scaling factor, *f*. The range explored is 1.2−1.6 with consideration of hybrid combinations of the extreme values. We recall that for $CH_3CN$, we have exploited a three-sphere cavity, in which the spheres are centered on the three heavy atoms with radii 1.55 Å for N, 1.7 Å for C (bonded to N), and 2.0 Å for methyl C.[26]

The first aspect to note looking at the results of Table 2 is the difficulty of the electrostatic-only continuum model to represent the apolar cyclohexane for which, at any cavity size, the computed solvent effect goes in the wrong direction indicating a shielding instead of the observed deshielding with respect to the gas phase. These findings confirm the considerations reported in the Introduction about limits of approximated approaches: for the apolar cyclohexane, in fact, an electrostatic-only model will hardly manage to reproduce the real effects (more likely produced by weak van der Waals forces); here, however, this problem will not be considered in more details as it is beyond the scope of the present paper.

More important for our scope is, in fact, the comparison between the two protic solvents, $CHCl_3$ and water. It seems clear that for both solvents, the standard 1.2 scaled cavity is not adequate, overestimating the solvent effect. Increasing the scaling factor, however, does not have the same effect in the two solvents: while for water 1.4 is enough to approach the experimental value, for $CHCl_3$, neither the largest value 1.6 nor any combinations of it is sufficient to properly reduce the final effect in agreement with experiments. The different behavior found in the two protic solvents confirms what was discussed in the Introduction about the reasons we have chosen $CHCl_3$ as test solvent. The highly polar character of water can in fact be well modelized in terms of electrostatic continuum models and also the strong H-bond it forms with the nitrogen atom can be taken into account by slightly enlarging the standard cavity as confirmed by the good value obtained with the last hybrid cavity in which only the N-centered sphere has been enlarged.

*3.2.2 Supermolecule Calculations.* The results obtained by exploiting an electrostatic-only continuum model have shown the necessity of introducing other interactions, in particular those deriving from short-range specific effects induced by H-bonding.

To get an accurate description of H-bond effects on nuclear shielding, a possible approach is through clusters formed by solute and some solvent molecules. For weak H-bonds as those formed by $CHCl_3$ however, the structure of such clusters is preferably obtained through MD simulations rather than through ab initio geometry optimizations. The weak character of this interaction in fact cannot be well represented in terms of a single rigid structure obtained as the minimum of the potential energy surface of the cluster. On the contrary, the real situation is dynamic and a variety of different and representative structures can and do occur. Here, this situation is achieved by considering structures derived from MD shots taken at different simulation times (see section 2 for details). In particular, we have used two sets of 10 structures including a variable number of solvent molecules: for each structure, the number of solvent molecules is determined by the threshold ($r_{cut}$) imposed in the distance between the acetonitrile N atom and the H of $CHCl_3$ (the number of these selected molecules varies from 1 to 4). For each structure of each set, we have computed two calculations, one in the gas phase and the other in the presence of an external continuum solvent mimicking the bulk $CHCl_3$. The calculations on clusters have been obtained exploiting the MO:MO ONIOM method implemented in the Gaussian code.

The ONIOM hybrid method is very general and can integrate any two (or more) computational methods. For a two-level ONIOM computation, the total energy of the system is obtained from three independent calculations:

$$E^{ONIOM} = E^{low,real} - E^{low,model} + E^{high,model}$$

where real denotes the full system, which is treated at the low computational level, while model denotes the part of the system for which the energy needs to be calculated at both the high and low level. The definition of the layers is rather straight-

**TABLE 3: ONIOM (B3LYP/6-311+G(d,p) and HF/STO-3G) N Nuclear Shielding, $\sigma$(N) (in ppm), of Acetonitrile in $CHCl_3$ Solution[a]**

| | VAC | | IEF−PCM | |
|---|---|---|---|---|
| | $\sigma$(N) | sd | $\sigma$(N) | sd |
| | | Flexible | | |
| set 1 | −19.52 | 8.45 | −8.31 | 7.48 |
| set 2 | −22.39 | 8.77 | −11.03 | 8.17 |
| average | −20.96 | | −9.67 | |
| | | Rigid | | |
| set 1 | −19.42 | 3.27 | −8.37 | 2.76 |
| set 2 | −20.95 | 2.57 | −9.10 | 1.98 |
| average | −20.18 | | −8.73 | |

[a] Sets 1 and 2 Refer to Two Different Sets of $CH_3CN(CHCl_3)_n$ Clusters Obtained from MD Simulations. The Column Labeled as "sd" Reports Values of Standard Deviation for Each of the Set of Clusters.

forward in our case as we do not have any covalent bond between the solute and the solvent molecules, the model being represented by $CH_3CN$ only. Besides the energy and its geometrical derivatives, other properties are available in the ONIOM framework as well:[29] here, in particular, we shall consider the isotropic shielding for which the integrated value can be calculated with an expression analogous to the ONIOM energy expression:

$$\sigma^{\mathrm{ONIOM}} = \sigma^{\mathrm{low,real}} - \sigma^{\mathrm{low,model}} + \sigma^{\mathrm{high,model}}$$

The ONIOM scheme has been recently generalized to include the IEF−PCM solvation model;[30] in this case, the two model calculations are computed keeping fixed the molecular cavity of the full real system (i.e., the whole cluster) but recomputing the reaction field in each subcalculation. Other ONIOM + IEF−PCM schemes have been formulated and implemented in a development version of the Gaussian code, but we have not tested them in the present study.

For any ONIOM calculation, the two levels of calculation employed are B3LYP/6-311+G(d,p) and HF/STO-3G. The validity of this combination has been tested on some selected clusters for which a full high-level calculation has been repeated both in gas phase and in solution. In all cases, the mean differences obtained between ONIOM and complete nuclear shieldings are around 1 ppm in gas phase and around 2 ppm in solution; these values can be thus assumed as the uncertainty range of our calculations.

Nitrogen isotropic shieldings, $\sigma$(N), obtained from ONIOM supermolecule calculations are reported in Table 3. The data are divided into two main groups depending on the type of models, rigid or flexible, used in the MD simulations. Each group is composed of two sets of 10 clusters selected as described above and used to compute N nuclear shieldings with and without adding an external continuum dielectric within the framework of the IEF−PCM. The computed shieldings of each set of 10 structures (which are not reported) have been arithmetically averaged to give the value reported in Table 3. A further average has been done between these two values; this is indicated as average. In the same table, for each set of clusters, we also report the standard deviation (sd).

As a first analysis, we consider the differences obtained by using the two alternative models for $CH_3CN$, i.e., the flexible and the rigid ones. From the sd values obtained, it is evident that the results from the flexible model are by far more sparse than those obtained keeping geometries fixed. This significant difference between the two models can be explained by recalling the high sensitivity of nuclear shielding on molecular geometries; also, small differences in bond lengths and angles can induce large variations in $\sigma$. The main aspect to note, however, is that the final mean value is very similar in the two models. This result gives us some level of confidence in the number of necessary structures to produce meaningful estimations and, therefore, in the validity of our analysis.

**TABLE 4: ONIOM (B3lyp/6-311+G(d,p) and HF/STO-3G) Gas-to-Solution Shift, $\Delta\sigma$(N) (in ppm), on N Nuclear Shielding of Acetonitrile in $CHCl_3$ Solution[a]**

| | Flexible | |
|---|---|---|
| | cluster | cluster + IEF |
| set 1 | −5.99 | −17.19 |
| set 2 | −3.12 | −14.48 |
| average | −4.56 | −15.84 |

| | Rigid | | | | |
|---|---|---|---|---|---|
| | cluster | | cluster + IEF | | |
| | | C···Cl | $f = 1.2$ | $f =$ mix | C···Cl |
| set 1 | −6.08 | | −17.15 | −13.10 | |
| set 2 | −4.56 | −5.35 | −16.41 | −11.83 | −12.15 |
| average | −5.32 | | −16.78 | −12.47 | |

[a] The experimental shift is −6.2 ppm (ref 6).

By comparing results obtained with flexible and rigid models, one could try to derive some qualitative considerations on vibrational contributions to the shielding. The similar results obtained with the two models, in fact, seem to indicate that nuclear vibrations do not affect too much the properties when taken as an averaged effect, even though the high sd value obtained for the flexible model confirms the sensitivity of the property to geometry effects. More detailed analyses on this point are required to get more stated conclusions, but as concerns the present paper, we limit ourselves to underline the problem without giving further comments.

To have a more direct comparison with experimental data, in Table 4, we report the computed variations of the isotropic shielding with respect to the value of the isolated molecule. The labels used to indicate the various models are the same as for the previous table, except we have added two new values for the rigid group of data. These have not been reported in the previous table as they are almost identical to the others with respect to the statistical analysis. The first new item regards IEF−PCM calculations and refers to a different definition of the cavity size used for the cluster: for the spheres centered on the two carbons of $CH_3CN$, we have used 1.6 as a scaling factor instead of the standard 1.2 value. The results obtained with this enlarged cavity are indicated as $f =$ mix ($f = 1.2$, on the contrary, refers to standard cavities). The second new value reported in Table 4 refers to enlarged clusters obtained from the set of MD configurations previously used in the set 2 by including additional solvent molecules. These larger clusters are built by adding a new cutoff distance for the pair Cl−methyl C of $CH_3CN$. In this case, RDFs centered in the methyl C atom show a preferential orientation of the chloroform molecules located in the neighborhood of the methyl group, in which chlorine atoms interact with the hydrogens of the $CH_3$ group. The cutoff distance used was 5.2 Å. So, any chloroform molecule satisfying one or both of the distance criteria was selected for the corresponding cluster. Figure 4 shows one of the used clusters in which it is possible to observe how the new criterion roughly allows the inclusion of a complete first solvation shell (eight to nine solvent molecules) around the acetonitrile molecule.

Taking into account the results shown in Table 3 and the considerable increase in the computational effort for the new

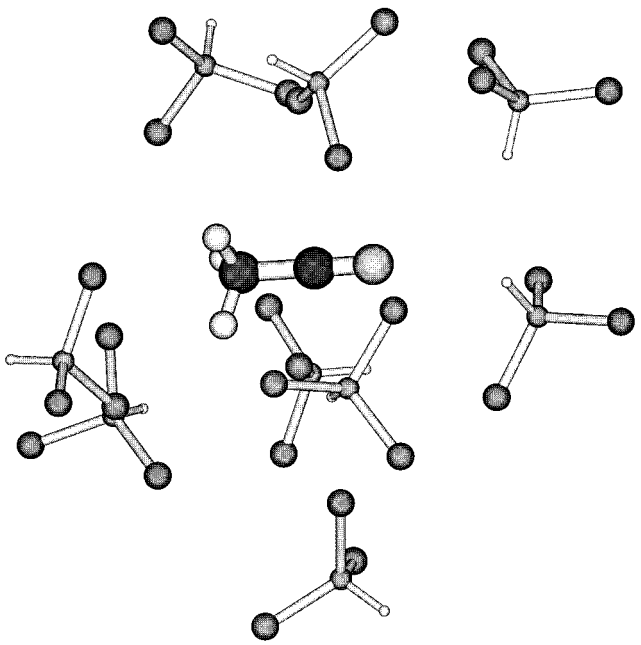

**Figure 4.** One of the structures used in the ONIOM computations of the C···Cl set (see text for details).

clusters because of the larger number of solvent molecules, the analysis will be limited to one of the two previously used sets and will be labeled as C···Cl.

The most important result from the data in Table 4 is that calculations on the clusters give very good mean $\Delta\sigma$(N) values (−4.56 ppm for the flexible model and −5.32 ppm for the rigid one vs the experimental −6.2 ppm) if performed in vacuo, while the agreement with experiments becomes much worse if we include the effects of an external continuum dielectric. By comparison of the final mean $\Delta\sigma$(N) of −16.78 ppm with the corresponding value of Table 2, obtained for the simple solute-only model, it seems that the electrostatic long-range interactions induced by the continuum dielectric are not significantly modified by the partial screening due to the explicit solvent molecules near the nitrogen atom, and indeed, the final IEF−PCM result still presents an overestimated shielding effect (more than twice the observed value).

The most striking fact is that neither the increase of the screening obtained by additional explicit solvent molecules around the solute (see C···Cl in Table 4) nor the enlargement of the cavity (see $f$ = mix in Table 4) can reduce this excessive electrostatic effect induced by the continuum. As a matter of fact, these two modifications have the same final effect of reducing the gas-to-solution computed shift of ∼5 ppm but still keeping it too large with respect to the observed value.

**3.3 Pyridine.** The analysis done on acetonitrile has shown some significant limits of continuum solvation models even when coupled to discrete approaches. Easy generalizations to other molecular systems should, however, be confirmed by numbers. Here, in particular, we present a molecule for which the results are completely different.

In Table 5, we report computed nuclear isotropic shieldings and computed and experimental gas-to-solution shifts for nitrogen of pyridine; the computed results refer to B3LYP/6-311+G(d,p) calculations exploiting the same experimental geometry for both gas-phase and solvated systems. Once again, calculations in solution have been performed within the IEF−PCM electrostatic continuum model; this time the molecular cavity has been obtained by interlocking six spheres centered

**TABLE 5: B3LYP/6-311+G(d,p) Nuclear Shielding (in ppm) and Gas-to-Solution Shift, $\Delta\sigma$(N), (in ppm) on Nitrogen of Pyridine**

| | | $\Delta\sigma$(N) | |
|---|---|---|---|
| | $\sigma$(N) | calcd | exptl[a] |
| vac | −102.78 | 0.0 | 0.0 |
| cyclohexane | −95.50 | −7.28 | −3.1 |
| $CHCl_3$ | −88.81 | −13.97 | −14.1 |
| water | −82.49 | −20.29 | −29.7 |

[a] Reference 6.

on each heavy atom with radii equal to 1.55 and 2.0 for N and C, respectively (all radii have been scaled by the standard 1.2 value).[26]

By comparing results of Table 5 with the corresponding ones obtained for acetonitrile (see Table 2), it comes out that for pyridine, the continuum solvation model behaves significantly better for all different solvents. When the experimental shifts of pyridine and acetonitrile are analyzed, it seems that these different performances of the solvation model obtained for the two molecules might be related to a larger contribution of electrostatic interactions in gas-to-solution shift in pyridine. For this molecule, in fact, all three solvents present a negative shift, while in acetonitrile, the apolar cyclohexane was characterized by a positive shift. In addition, the magnitude of the shifts well correlate with the dielectric constant of each solvent thus indicating the leader role acted by electrostatic interactions. Clearly, also, other nonelectrostatic interactions are effective, and in fact, for cyclohexane, the computed shift is overestimated indicating the necessity to introduce other effects related to van der Waals interactions. In water, on the contrary, the computed shift is too low as this time the main missing term is that due to H-bond specific effects. The intermediate position of $CHCl_3$, both as concerns its polarity and its capability to do H-bonds, leads to a very good agreement between computed and experimental shifts; in this case, in fact, it seems very probable that the computed electrostatic effects, slightly overestimated as in cyclohexane, manage to compensate for the missing effects due to H-bonding on one hand and van der Waals interactions on the other hand.

This analysis can be further tested by applying the same approach used for acetonitrile; here, it is not worth reporting the effects of changes in the cavity size (as done in Table 2 for acetonitrile) as the results obtained with the standard cavity (i.e., with a scaling factor $f$ equal to 1.2) clearly show that an eventual enlargement of the cavity can only lead to a regular decrease of the solvent effects.

Let us, on the contrary, repeat the analysis on clusters. As was done for acetonitrile, for pyridine, we extract two sets of 10 solute−solvent cluster structures from MD simulations on which we compute the isotropic shielding (details in section 2) and the following averaging. The results obtained for the isolated clusters and for the same clusters immersed in an external continuum dielectric are reported in Table 6.

The comparison between clusters in vacuo and in a continuum dielectric confirms our analysis on the important contribution of the long-range electrostatic forces. The isolated clusters, in fact, do not manage to account for the whole solvent effect, and the corresponding shift is too small; including the additional interactions due to the bulk (i.e., introducing an external continuum) immediately recovers the complete effect (we recall that the intrinsic uncertainty of these calculations is around 2 ppm). In this case, long-range electrostatic forces and short-range and directional H-bonds can be algebraically summed to give the final global effect.

**TABLE 6: ONIOM (B3LYP/6-311+G(d,p) and HF/STO-3G) Nuclear Shielding (in ppm) and Gas-to-Solution Shift ($\Delta\sigma$(N)) on N of Pyridine in $CHCl_3$ Solution[a]**

| | cluster | | cluster + IEF | |
|---|---|---|---|---|
| | $\sigma$(N) | $\Delta\sigma$(N) | $\sigma$(N) | $\Delta\sigma$(N) |
| set 1 | −95.62 | −7.16 | −87.89 | −14.89 |
| set 2 | −93.10 | −9.68 | −86.26 | −16.52 |
| average | −94.63 | −8.42 | −87.07 | −15.70 |

[a] Set 1 and 2 Refer to Two Different Sets of Py$(CHCl_3)_n$ Clusters Obtained through MD simulations.

**3.4. Paramagnetic Shielding and NBO Analysis.** It has been observed (and our calculations confirm these findings) that chemical-shift trends for nitrogen nuclei in different environments arise almost entirely from variations in the local paramagnetic shielding contribution, the corresponding local diamagnetic term being effectively constant.

To interpret the local paramagnetic contribution in terms of computed electronic properties, Pople[27] developed a shielding model in which variations in nuclear shielding are related to changes in local charge densities, bond orders, and the energy of electronically excited states. In its most used version, Pople's shielding model relies upon the average excitation energy (AEE) approximation; by this means, the local paramagnetic shielding term for nucleus A becomes

$$\sigma_A^P(\mathrm{loc}) = -\frac{\mu_0\hbar^2e^2}{8\pi m^2}\frac{1}{\Delta E}\langle r^{-3}\rangle_{2p}\sum_B Q_{AB} \qquad (8)$$

where the summation over nucleus B includes A and $Q_{AB}$ involves elements of the charge density−bond order matrix, $\Delta E$ is the AEE, and $\langle r^{-3}\rangle_{2p}$ is the mean inverse cube of the radius of the 2p orbitals on the atom containing nucleus A.

From the equation above, it is possible to interpret nitrogen shielding variations in the light of a dominant change in the charge density and/or electronic excitation energy. Actually, the presence of the $\Delta E$ factor arises from the use of second-order perturbation theory in the development of the expression for the local paramagnetic shielding term; in other words, it is more a consequence of the quantum mechanical method rather than a parameter bearing a direct relationship to experimentally observable electronic transitions.

If now we apply this scheme to the interpretation of H-bond effects on nitrogen shielding, two classes of environments can be identified: in one class, the N lone-pair electrons are directly involved in the H-bonds and a $\pi$-electron system is available for low-energy n $\rightarrow \pi^*$ transitions to be considered as possible contributions to the paramagnetic shielding term. The effective removal of the lone pair from the nitrogen atom eliminates the n $\rightarrow \pi^*$ contribution such that the paramagnetic term is reduced in magnitude and an increase in the total nuclear shielding occurs. Examples of this category are cyanides, imines, and pyridine-type nitrogens. The second class of nitrogen environments, which we quote just for the sake of completeness but do not deal with, comprises those where the N lone-pair electrons may not be directly involved in H-bonding and/or there is no suitable $\pi$ system available for n $\rightarrow \pi^*$ contributions to be worthy of consideration. In such cases, H-bond formation could lead to an increase in the $\langle r^{-3}\rangle$ term in the equation of the local paramagnetic term and thus to an overall shielding decrease. Behavior of this kind is expected for amides, isonitriles, and most alkylamines.

To rationalize the presented results according to this interpretative scheme, we have focused on the paramagnetic contribution to the shielding, $\sigma^p$. In particular, we have tried to relate $\sigma^p$ to the net atomic charge as proposed by Karplus and Pople[32] many years ago. Natural bond orbital (NBO) analysis[33] will be used here for that purpose.

**TABLE 7: Isotropic Paramagnetic Shielding (ppm), Natural Atomic Charge (NAC), and Total Valence Population (NP) (au) on Nitrogen of Acetonitrile in the Isolated (M) and Solvated (M + IEF) Molecule and in the Selected Set of Clusters without (C) or with (C + IEF) Addition of an External Continuum Dielectric**

| | $\sigma^p$(N) | NAC | NP |
|---|---|---|---|
| M | −358.73 | −0.3400 | 5.3199 |
| M + IEF | −341.17 | −0.4100 | 5.3891 |
| C | −354.32 | −0.3714 | 5.3485 |
| C + IEF | −343.28 | −0.4151 | 5.3917 |

**TABLE 8: Diagonal Components of the Paramagnetic Shielding Tensor and 2p Natural Atomic Orbital Occupancies for N Atom in Acetonitrile**

| | $\sigma^p_{xx}$(N) | $\sigma^p_{zz}$(N) | $2p_x$ | $2p_z$ |
|---|---|---|---|---|
| M | −522.82 | −30.98 | 1.1039 | 1.5289 |
| M + IEF | −497.43 | −29.05 | 1.1356 | 1.5384 |
| C | −352.03 | −382.49 | 1.2187 | 1.2344 |
| C + IEF | −340.54 | −333.29 | 1.2380 | 1.2912 |

This analysis has been limited to a single set of clusters for both solutes (namely set 2 of the rigid model), for which we have computed the paramagnetic shielding tensor and the natural population analysis.

Starting from acetonitrile, the mean data for the selected set of clusters (C), also including an external continuum (C + IEF), are reported in Table 7 together with the parallel results obtained for the single molecule in gas phase (M) and in solution (M + IEF).

From the results in Table 7, the linear relationship between isotropic paramagnetic shielding and natural atomic charge (nuclear charge minus summed natural populations of NAOs) on nitrogen atom becomes evident, as well as its dependence on the valence natural population. The increase of electron population on the nitrogen atom (i.e., a more negative natural charge) passing from the isolated molecule to the solvated system ( described as IEF solvated molecule or cluster) can be explained in terms of a charge separation in C−N triple bond which, leading to a larger dipole moment, further stabilizes the solvated molecule because of the solute−solvent interactions.

These solvent-induced changes can be quantified in terms of the increase in the valence natural population which, in turn, linearly depends on the 2p natural atomic orbital occupancy. For a more detailed analysis of this point, in Table 8, we report the diagonal components of the paramagnetic shielding tensor ($\sigma_{yy}$ is not reported as parallel to $\sigma_{xx}$) and the $2p_x$ and $2p_z$ orbital occupancies.

The data reported in Table 8 can be used to quantify different effects. If we first focus on H-bonds, we see that passing from the single molecule (isolated or surrounded by a continuum dielectric) to the clusters, the $2p_z$ electron occupancy is strongly decreased due to electron donation from N to H (here the CN bond, and thus the nitrogen lone pair, is along $z$ axis). This electron charge transfer is reflected in the $\sigma^p_{zz}$ values as predicted by eq 8; removing the electron population from an orbital allows the corresponding electron orbit to shrink toward the nucleus increasing the $\langle r^{-3}\rangle$ term and thus the magnitude of the paramagnetic contribution. An opposite trend, even if of smaller magnitude, is observed for the $2p_x$ (and $2p_y$) orbitals and the corresponding $\sigma^p_{xx}$(N); adding H-bonding effects leads to larger occupancies and smaller shieldings.

**TABLE 9: Diagonal Components of the Paramagnetic Shielding Tensor and 2p Natural Atomic Orbital Occupancies of N Atom in Pyridine**

| | $\sigma^{p}_{xx}$(N) | $\sigma^{p}_{zz}$(N) | $2p_x$ | $2p_z$ |
|---|---|---|---|---|
| M | −567.09 | −692.29 | 1.5560 | 1.3361 |
| M + IEF | −553.70 | −661.60 | 1.5624 | 1.3415 |
| C | −554.90 | −668.10 | 1.5579 | 1.3407 |
| C + IEF | −548.70 | −653.60 | 1.5611 | 1.3434 |

A further effect to be considered is that due to electrostatic long-range interactions induced by the continuum dielectric which leads to a larger occupancy of all 2p orbitals with respect to the isolated systems (either the single molecule or the cluster). This result seems to indicate that at least for this solute−solvent couple, solvation continuum models fail as electrostatic effects are less important than and not completely coherent with those due to H-bonds. The latter cannot be properly represented in a continuum framework; this, in fact, cannot reproduce the anisotropic field required to describe the strongly localized and directional N···H interaction. Also, in the presence of discrete solvent molecules which should account for the H-bond part of the interaction, the inclusion of the strong long-range electrostatic forces due to the continuum destroys the anisotropic field produced by these solvent molecules leading to a wrong global effect.

The interesting results obtained for acetonitrile have led us to try to apply the same scheme of analysis to the completely opposite behavior shown by pyridine. Following the previous analysis on the dependence of solvent-induced changes of N nuclear shielding of acetonitrile on the 2p natural atomic orbital occupancy, in Table 9, we report the diagonal components of the paramagnetic shielding tensor ($\sigma_{yy}$ is not reported as it is small and almost constant) and the $2p_x$ and $2p_z$ orbital occupancies for the cluster in gas phase (C) and in the continuum (C + IEF). We recall that in this case, the molecule is assumed to lie on the *xz* plane with an angle of 30° between *z* and N−C (in para) axes.

From data of Table 9, it appears very clearly that this time, H-bond effects are weak or at least less important than the electrostatic interactions. This can be proved by two different results. On one hand, H-bond effects cannot be very effective, as passing from the isolated molecule (M) to the clusters (C), we observe only a slight increase of both 2p orbital occupancies (here, both orbitals should be involved in the H-bond because of the orientation of the molecule with respect to the Cartesian axes); on the contrary, for $CH_3CN$, a significant decrease in the $2p_z$ orbital (in this case the only one directly involved in H-bonding) was found. On the other hand, the electrostatic effects seem to be dominant as by including solvent effects either as a continuum or a cluster, very similar results are found (even if the isolated clusters, i.e., the discrete solvent molecules alone, produce smaller changes). Both observations seem to clarify many aspects of the very different behavior shown by pyridine with respect to acetonitrile and to confirm the validity of the interpretative scheme we have formulated in terms of the relative importance of H-bond and electrostatic effects.

## 4. Conclusions

The high sensitivity of nuclear shieldings to the natural environment of the selected nucleus (i.e., the other atoms forming the molecule and the way these are bonded but also the external surrounding) makes it one of the best properties to test theoretical solvation models. The studies in this direction that have appeared so far in the literature give a spectrum of examples and of computational methods showing very different performances (see previously cited papers and ref 34 for a list of additional references). In any case, however, very few efforts have been devoted to a real rationalization of the results; an important exception to this generalized trend is represented by the work of Witanowski and co-workers,[35] who have investigated solvent-induced variations in N shieldings of many molecular systems both in terms of an empirical scheme (that proposed by Kamlet, Taft, and co-workers[36]) to quantify the relative importance of the various components of such effects and in terms of semiempirical calculations using the solvaton model to numerically evaluate the solvent polarity contribution.

With the present paper, we have tried to begin a new procedure which involves, at first, a detailed numerical analysis through different theoretical approaches and their coupling and, second, an analysis of the numerical results in terms of interpretative tools derived from the same ab initio calculations (here the NBO analysis). This scheme should allow not only experience on the best way to compute a complex property like magnetic shielding through ab initio calculations including the effect of the solvent but also a deeper understanding of the intermolecular interactions acting in a liquid phase and the way these can be modelized through theoretical methods.

More particularly, our analysis has been focused on the competitive effects due to short-range and highly localized (and directional) H-bonds, on one hand, and those due to long-range and averaged electrostatic forces, on the other hand. Other possible interactions, such as those related to van der Waals forces, and/or other specific effects of magnetic properties, such as the so-called aromatic solvent-induced shift (ASIS effects),[37] have not been considered here. In particular, they have been avoided through the preliminary selection of the couple solute−solvent. Within this specific and restricted window of analysis, in fact, the most important interactions can be more easily identified and accurately included in the computations through both continuum and discrete solvation approaches, as well as their combination.

The combined use of classical statistical simulations with quantum chemistry techniques is becoming an efficient approach to overcome the limitations associated with the existence of several representative minima in the potential energy surface. This fact is particularly true in liquid solutions, such as that of acetonitrile or pyridine in $CHCl_3$, with moderate to low solute−solvent and solvent−solvent interactions. One of the most followed coupling schemes is the use of structures classically generated in high-level quantum chemical calculations in the gas phase. In this work, an extension of this scheme has been used in which supermolecule calculations are completed with a continuum model to include the long-range electrostatic effects which are missing in simple gas-phase clusters.

The results here presented show how this coupling is far from being easily applied and even completely understood when the study is performed on a complex property like the nuclear shielding here considered. Further work in this sense must be done in several ways.

From the point of view of the generation of the "best" clusters, the effect of using different potentials must be studied in order to state the possible influence in the final estimations of the classically generated ensembles. Our results seem to indicate that the use of rigid models can produce equivalent results when compared to those obtained with flexible, and more complex, force fields in the case of small and relatively rigid solutes such as acetonitrile. However, the validity of this statement for larger and more flexible solutes must be studied.

From the complementary point of view of a possible improvement of continuum models, the results obtained for acetonitrile give a clear and strong signal that things are more complex than what one can predict from the simple consideration of the intermolecular forces as a sum of additive effects. In other words, the widespread idea that results will become automatically more and more accurate just by including a larger number of interactions in the model from whatever physical model they are obtained has to be accepted with care; competitive effects, in fact, if not computed in a coherent way (same level of calculation and same modelistic approach), can wrongly combine to give a final overestimated (or underestimated) effect.

**Acknowledgment.** J.M.M. thanks the Ministerio de Educación y Cultura (M.E.C.) of Spain for a postdoctoral fellowship.

## References and Notes

(1) (a) Buckingham, A. D. *Can. J. Chem.* **1960**, *38*, 300. (b) Buckingham, A. D.; Schaefer, T.; Schneider, W. G. *J. Chem. Phys.* **1960**, *32*, 1227.

(2) (a) Chesnut, D. B.; Rusiloski, B. E. *J. Mol. Struct.: THEOCHEM* **1994**, *314*, 19. (b) Hinton, J. F.; Guthrie, P.; Pulay, P.; Wolinski, K. *J. Am. Chem. Soc.* **1992**, *114*, 1604. (c) Pecul, M.; Sadlej, J. *Chem. Phys.* **1998**, *234*, 111.

(3) Mikkelsen, K. V.; Jørgensen, P.; Ruud, K.; Helgaker, T. *J. Chem. Phys.* **1997**, *106*, 1170.

(4) (a) Cremer, D.; Olsson, L.; Reichel, F.; Kraka, E. *Isr. J. Chem.* **1993**, *33*, 369. (b) Zhan, C. G.; Chipman, D. M. *J. Chem. Phys.* **1990**, *110*, 1611.

(5) (a) Cammi, R. *J. Chem. Phys.* **1998**, *109*, 3185. (b) Cammi, R.; Mennucci, B.; Tomasi, J. *J. Chem. Phys.* **1999**, *110*, 7627.

(6) Witanowski, M.; Stefaniak, L.; Webb, G. A. In *Annual Reports on NMR Spectroscopy*; Webb, G. A., Ed.; Academic Press: London, 1993; Vol. 25.

(7) (a) Miertus, S.; Scrocco, E.; Tomasi, J. *Chem. Phys.* **1981**, *55*, 117. (b) Cammi, R.; Tomasi, J. *J. Comput. Chem.* **1995**, *16*, 1449.

(8) (a) Hameka, H. F. *Rev. Mod. Phys.* **1962**, *34*, 87. (b) Ditchfield, R. *Mol. Phys.* **1974**, *27*, 789. (c) Wolinski, K.; Hinton, J. F.; Pulay, P. *J. Am. Chem. Soc.* **1990**, *112*, 8251.

(9) (a) Cancès, E.; Mennucci, B. *J. Math. Chem.* **1998**, *23*, 309. (b) Cancès, E.; Mennucci, B.; Tomasi, J. *J. Chem. Phys.* **1997**, *107*, 3031. (c) Mennucci, B.; Cancès, E.; Tomasi, J. *J. Phys. Chem. B* **1997**, *101*, 10506.

(10) Forrester, T. W.; Smith, W. *DL_POLY*, version 2.12; CCLRC, Daresbury Laboratory: Daresbury, England, 1995.

(11) Fox, T.; Kollman, P. A. *J. Phys. Chem. B* **1998**, *102*, 8070.

(12) Grabuleda, X.; Jaime, C.; Kollman, P. *J. Comput. Chem.* **2000**, *21*, 901.

(13) Cornell, W.; Cieplak, P.; Baylay, C. I.; Gould, I. R.; Merz, K. R., Jr.; Ferguson, D. M.; Spellmeyer, D.; Fox, T.; Caldwell, J.; Kollman, P. *J. Am. Chem. Soc.* **1995**, *117*, 5179.

(14) Ryckaert, J.; Ciccotti, G.; Berendsen, H. *J. Comput. Phys.* **1977**, *23*, 327.

(15) Jorgensen, W. L.; McDonald, N. A. *J. Mol. Struct.: THEOCHEM* **1998**, *424*, 145.

(16) Goldstein, H. *Classical Mechanics*, 2nd ed.; Addison-Wesley: Reading, MA, 1980.

(17) Fincham, D. *Mol. Simul.* **1992**, *8*, 165.

(18) Allen, M.; Tildesley, D. *Computer Simulations of Liquids*; Clarendon Press: Oxford, U.K., 1989.

(19) *CRC Handbook of Chemistry and Physics*; Weast, R. C., Ed.; CRC Press: Boca Raton, FL, 1988.

(20) (a) Cheeseman, J. R.; Trucks, G. W.; Keith, T. A.; Frisch, M. J. *J. Chem. Phys.* **1996**, *104*, 5497. (b) Johnson, B. G.; Frisch, M. J. *J. Chem. Phys.* **1994**, *100*, 7429.

(21) Frisch, M. J.; Trucks, G. W.; Schlegel, H. B.; Scuseria, G. E.; Robb, M. A.; Cheeseman, J. R.; Zakrzewski, V. G.; Montgomery, J. A., Jr.; Stratmann, R. E.; Burant, J. C.; Dapprich, S.; Millam, J. M.; Daniels, A. D.; Kudin, K. N.; Strain, M. C.; Farkas, O.; Tomasi, J.; Barone, V.; Cossi, M.; Cammi, R.; Mennucci, B.; Pomelli, C.; Adamo, C.; Clifford, C. S.; Ochterski, J.; Petersson, G. A.; Ayala, P. Y.; Cui, Q.; Morokuma, K.; Malick, D. K.; Rabuck, A. D.; Raghavachari, K.; Foresman, J. B.; Cioslowski, J.; Ortiz, J. V.; Stefanov, B. B.; Liu, G.; Liashenko, C. A.; Piskorz, P.; Komaromi, I.; Gomperts, R.; Martin, R. L.; Fox, D. J.; Keith, T.; Al-Laham, M. A.; Peng, C. Y.; Nanayakkara, A.; Gonzalez, C.; Challacombe, M.; Gill, P. M. W.; Johnson, B.; Chen, W.; Wong, M. W.; Andres, J. L.; Head-Gordon, M.; Replogle, E. S.; Pople J. A. *Gaussian 99*, development version; Gaussian, Inc.: Pittsburgh, PA, 1999.

(22) Adamo, C.; Barone, V. *J. Chem. Phys.* **1998**, *108*, 664. (b) Perdew, J. P.; Burke, K.; Wang, Y. *Phys. Rev. B* **1996**, *54*, 16533.

(23) Wiberg, K. *J. Comput. Chem.* **1999**, *20*, 1299.

(24) Tomasi, J.; Persico, M. *Chem. Rev.* **1994**, *94*, 2027.

(25) (a) Luque, F. J.; Bachs, M.; Aleman, C.; Orozco, M. *J. Comput. Chem.* **1996**, *17*, 806. (b) Chambers, C. C.; Hawkins, G. D.; Cramer, C. J.; Truhlar, D. G. *J. Phys. Chem.* **1996**, *100*, 16385. (c) Aguilar, M. A.; Olivares del Valle, F. J. *Chem. Phys.* **1989**, *129*, 439. (d) Barone, V.; Cossi, M.; Tomasi, J. *J. Chem. Phys.* **1997**, *107*, 3210.

(26) Bondi, A. *J. Phys. Chem.* **1964**, *68*, 441.

(27) Pople, J. A. *Discuss. Faraday Soc.* **1962**, *34*, 7.

(28) (a) Humbel, S.; Sieber, S.; Morokuma, K. *J. Chem. Phys.* **1996**, *16*, 1959. (b) Svensson, M.; Humbel, S.; Froese, R. D. J.; Matsubara, T.; Sieber, S.; Morokuma, K. *J. Phys. Chem.* **1996**, *100*, 19357.

(29) (a) Dapprich, S.; Komáromi, I.; Byun, K. S.; Morokuma, K.; Frisch, M. J. *J. Mol. Struct.: THEOCHEM* **1999**, *461*, 1. (b) Vreven, T.; Morokuma, K. *J. Comput. Chem.* **2000**, *16*, 1419. (c) Froese, R. D. J.; Morokuma, K. *Chem. Phys. Lett.* **1996**, *263*, 393. (d) Karadakov, P. B.; Morokuma, K. *Chem. Phys. Lett.* **2000**, *317*, 589. (e) Vreven, T.; Morokuma, K. *J. Chem. Phys.* **2000**, *113*, 2969.

(30) Vreven, T.; Mennucci, B.; da Silva, C. O.; Morokuma, K.; Tomasi, J. *J. Chem. Phys.* **2001**, *115*, 62.

(31) Nymand, T. M.; Åstrand, P.-O.; Mikkelsen, K. *J. Phys. Chem. B* **1997**, *101*, 4105.

(32) Karplus, M.; Pople, J. A. *J. Chem. Phys.* **1963**, *38*, 2803.

(33) Glendening, E. D.; Reed, A. E.; Carpenter, J. E.; Weinhold, F. *NBO*, version 3.1.

(34) Helgaker, T.; Jaszunski, M.; Ruud, K. *Chem. Rev.* **1999**, *99*, 293.

(35) (a) Witanovski, M.; Sicinska, W.; Webb, G. A. *Magn. Reson. Chem.* **1989**, *27*, 380. (b) Witanovski, M.; Sicinska, W.; Biernat, S.; Webb, G. A. *J. Magn. Reson.* **1991**, *91*, 289. (c) Witanovski, M.; Sicinska, W.; Webb, G. A. *J. Magn. Reson.* **1992**, *98*, 109. (d) Witanovski, M.; Bledrzycka, Z.; Sicinska, W.; Grabowski, Z.; Webb, G. A. *J. Magn. Reson.* **1997**, *124*, 127. (Just to cite those focused on the same, or related, molecules discussed in the present work.)

(36) Kamlet, M. J.; Abboud, J. L. M.; Taft, R. W. *Prog. Phys. Org. Chem.* **1980**, *13*, 485.

(37) Reichardt, C. *Solvents and Solvent Effects in Organic Chemistry*, 2nd ed.; VCH: New York, 1988.